www.czasopisma.pan.pl PAN www.journals.pan.pl
Chemical and Process Engineering 2022, 43 (1), 3–21
DOI: 10.24425/cpe.2021.138941

Image analysis framework for hydraulic mixing

Aleksandra Golczak, Waldemar Szaferski, Szymon Woziwodzki, Piotr T. Mitkowski*

Poznan University of Technology, Department of Chemical Engineering and Equipment, Berdychowo 4, 60-965 Poznan, Poland

This study is focused on the image analysis of motionless hydraulic mixing process, for which pressure changes were the driving force. To improve the understanding of hydraulic mixing, mixing efficiency was assessed with dye introduction, which resulted in certain challenges. In order to overcome them, the framework and methodology consisting of three main steps were proposed and applied to an experimental case study. The experiments were recorded using a camera and then processed according to the proposed framework and methodology. The main outputs from the methodology which were based only on the recorded movie were liquid heights and colour changes during the process time. In addition, considerable attention has also been given to issues related to other colour systems and the hydrodynamic description of the process.

Keywords: hydraulic mixing, image processing, analysis of mixing time, RGB colour model

1. INTRODUCTION

One of the main goals of modern chemical engineers is to intensify chemical and physical processes by means of heat, mass and momentum exchange. From the very beginning of development of chemical and process industries, obtaining the best and the most effective homogenization of multicomponent mixtures has always been a priority. Every year, innovative ways of mixing liquids with various physical and chemical parameters as well as unusual configurations of specialist and sophisticated equipment are proposed. Mixing may seem simple and not worth much attention, especially in case of liquid mixtures that are harmless for human health and the environment, which is reflected by a decreasing number of scientific publications in recent years. Nevertheless, the mixing of flammable, explosive or toxic substances is still associated with risk and research attention is targeted to motionless mixing strategies (Mitkowski et al., 2016).

Assessment of mixing, either qualitative or quantitative, is still troublesome and involves vast experimental and computational efforts. One of the oldest experimental methods for visualization of flow behaviour and effectiveness of mixing, which dates back to the 19th century (Reynolds, 1883) but is still widely used, is based on the application of dyes as mixing indicators (Ghanem et al., 2014; Hardt and Schönfeld, 2003; Mitkowski et al., 2016; Schönfeld et al., 2004; Woziwodzki, 2014). In general, the use of this technique requires a transparent apparatus, usually consisting of glass or plexiglass, and an injection place of dye. In

* Corresponding author, e-mail: piotr.mitkowski@put.poznan.pl

addition to the difficulties associated with building the transparent equipment, the assessment of colours causes great challenges.

Colour assessment can be carried out using various commercial, freeware and open source computer-aided tools. One of them is ImageJ, which is a freely available image processing program. The program is implemented in Java and allows to solve many problems related to image processing and analysis (Ferreira and Rasband, 2012). The software has been used in many scientific fields, including biological sciences for 3D imaging of living cells (Eliceiri and Rueden, 2005) and chemical engineering for the identification of Isolated Mixing Regions in a steady and unsteady mixing process (Woziwodzki, 2014). Other software used by researchers for image processing include Matlab, Image Processing Toolbox and Image Pro Plus.

Regardless of which software is considered, it deals with colour space models, which are called colour models in short. By definition, colour is a psychophysical feature of visual perception, which means that every person can interpret it in a different way. Colour analysis can be used in scientific research, therefore it should be presented in an objective manner, and it is necessary to use colour space models, such as RGB or CMYK model. The colour theory contains three parameters by which the colour can be unambiguously identified, namely: hue, saturation and brightness (Plataniotis and Venetsanopoulos, 2014).

The CMYK and RGB models belong to the type of device dependent models. Such graphic representations possess a disadvantage that makes the colour visually different depending on the device on which it will be displayed. However, both RGB and CMYK are widely used in computer graphics and can be used in colour analysis for research purposes (Bratkova et al., 2009; McAndrew, 2004). The models are characterized by ease of calculation and integration into the structure of popular graphic software, programming languages and software tools for supporting design (e.g. Adobe Photoshop, Adobe Illustrator, Corel Draw, ImageJ, Image Pro Plus, MATLAB, Python). The number of colours obtained in the CMYK model is lower than in the RGB model. CIELab is another widely used colour model. The CIELab model was created on the basis of statistical analysis of answers given by respondents and is described in literature as a standard observer model. Due to the focus on computer analysis in this work and the inability to integrate the CIELab colour space into the software used, the model will not be discussed here in more detail (Molenda et al., 2012).

The RGB name stands for colours forming the model, i.e. red, green and blue, and is the most widely used colour model (Jankowski, 2006). The RGB colour space is used by the majority of computer software (Afshari-Jouybari and Farahnaky, 2011). This is an additive model, hence in order to obtain a specific colour, individual components need to be combined until white light is obtained. The range of the model relates to intervals: 600÷700 nm red, 500÷600 nm green, 400÷500 nm blue (Plataniotis and Venetsanopoulos, 2014). The coordinates R, G and B take values from 0 to 255. All components with a value equal to 0 denote black, and those with a value equal to 255 represent white (Jankowski, 2006). In computer colour processing, each signal corresponding to a given coordinate is independently recorded and digitized (Bishop, 1992; Plataniotis and Venetsanopoulos, 2014).

The colour can be characterized by three parameters: hue, saturation and brightness. The hue is an angle determining the position of the colour on the well-known colour wheel. The symbolic beginning of the colour wheel is in a place equivalent to pure red and in the RGB model that colour will be marked as (1, 0, 0). A hue equal to zero denotes red. The hue value is marked with the letter H (Plataniotis and Venetsanopoulos, 2014). In order to calculate the hue value, the minimum and maximum value of the RGB components must be found. The next step determines the area to which the colour belongs, and finally the obtained values are substituted to Eq. (1).

$$\frac{\text{third} - \text{minimum}}{\text{maximum} - \text{minimum}} = \frac{\text{unknown hue} - \text{beginning of interval}}{\text{end of interval} - \text{beginning of interval}} \tag{1}$$

Saturation is indicated by the letter S and it is defined as the degree of mixing of the primary colour with white light. The colour becomes faded as the amount of white increases. Saturation can be represented by converting a chromatic colour to an achromatic one, i.e. to shades of grey. The colours which possess the first component in Eq. (2) are chromatic colours.

$$(\mathrm{R}, \mathrm{G}, \mathrm{B}) = (\mathrm{R} - m,\ \mathrm{G} - m,\ \mathrm{B} - m) + (m, m, m), \quad m = \min(\mathrm{R}, \mathrm{G}, \mathrm{B}) \tag{2}$$

Saturation is calculated based on a formula (Eq. (3)) and the result is always normalized to one and multiplied by the maximum resolution of the colour, i.e. 255 by default (Plataniotis and Venetsanopoulos, 2014).

$$\mathrm{S} = \frac{\max(\mathrm{R}, \mathrm{G}, \mathrm{B}) - \min(\mathrm{R}, \mathrm{G}, \mathrm{B})}{\max(\mathrm{R}, \mathrm{G}, \mathrm{B})} \tag{3}$$

Brightness is often confused with lightness, but these are two different parameters. Brightness is a change of colour lightness at which saturation remains unchanged. Lightness (L) is equal to 0 for black and maximum lightness represents fully saturated colours. Lightness is described by Eq. (4) (Plataniotis and Venetsanopoulos, 2014).

$$\mathrm{L} = \frac{\max(\mathrm{R}, \mathrm{G}, \mathrm{B}) + \min(\mathrm{R}, \mathrm{G}, \mathrm{B})}{2} \tag{4}$$

In the CMYK model, all available colours are created by subtracting red, green and blue colours from white by covering the printing substrate with the following component colours: blue-green (C), purple (M), yellow (Y), black (K, called the key colour). In the cube of the CMYK model, component K is the fourth dimension which is not presented. Note, that the CMYK model is sometimes called CMY (Galer and Horvat, 2003).

The gamuts of RGB and CMYK spaces differ significantly, as shown in the top part of Fig. 1. Most of the known graphic software include a simple RGB–CMYK conversion mechanism, which is performed by the colour management systems, using ICC profiles dedicated to specific devices. The graphical comparison of two space colour models and its limitation in conversion are presented in Fig. 1. The built-in software warnings addressed to the user in case the selected colour is outside the range of the CMYK model are another useful feature.

The objective of this work is to present the proposed framework and methodology of computer-aided image analysis for hydraulic mixing (CIA4HM). The process of hydraulic mixing was described in detail elsewhere (Mitkowski et al., 2016) along with the manual-like method of image analysis. The CIA4HM analysis utilizes the RGB colour space model, which was selected because of its integration into the applied software, i.e. Matlab and MS Excel (Vega-Alvarado et al., 2011). The important advantage of using the RGB model is the recording of colour in the form of three independent components. This allows to obtain more accurate results and to use the formulas for calculation of the basic characteristic colour parameters, such as hue, saturation and brightness (Cabaret et al., 2007). The important outputs of the presented methodology of image analysis are that the duration of the analysis, which lasted up to several days in case of the manual-like method, is reduced to approx. 60 minutes and that the assessment of colour change is human independent.

2. EXPERIMENTAL SET-UP AND ITS CHARACTERISTICS

All the experimental data presented in this study have been obtained using the unique experimental set-up of a hydraulic mixer (HM). The scheme of the experimental set-up is presented in Fig. 2 which is working in a cycle mode according to process step specification presented schematically in Fig. 3. The working cycle of the HM consisted of cyclic changes of pressure, due to cyclic in and out gas flow from inner and

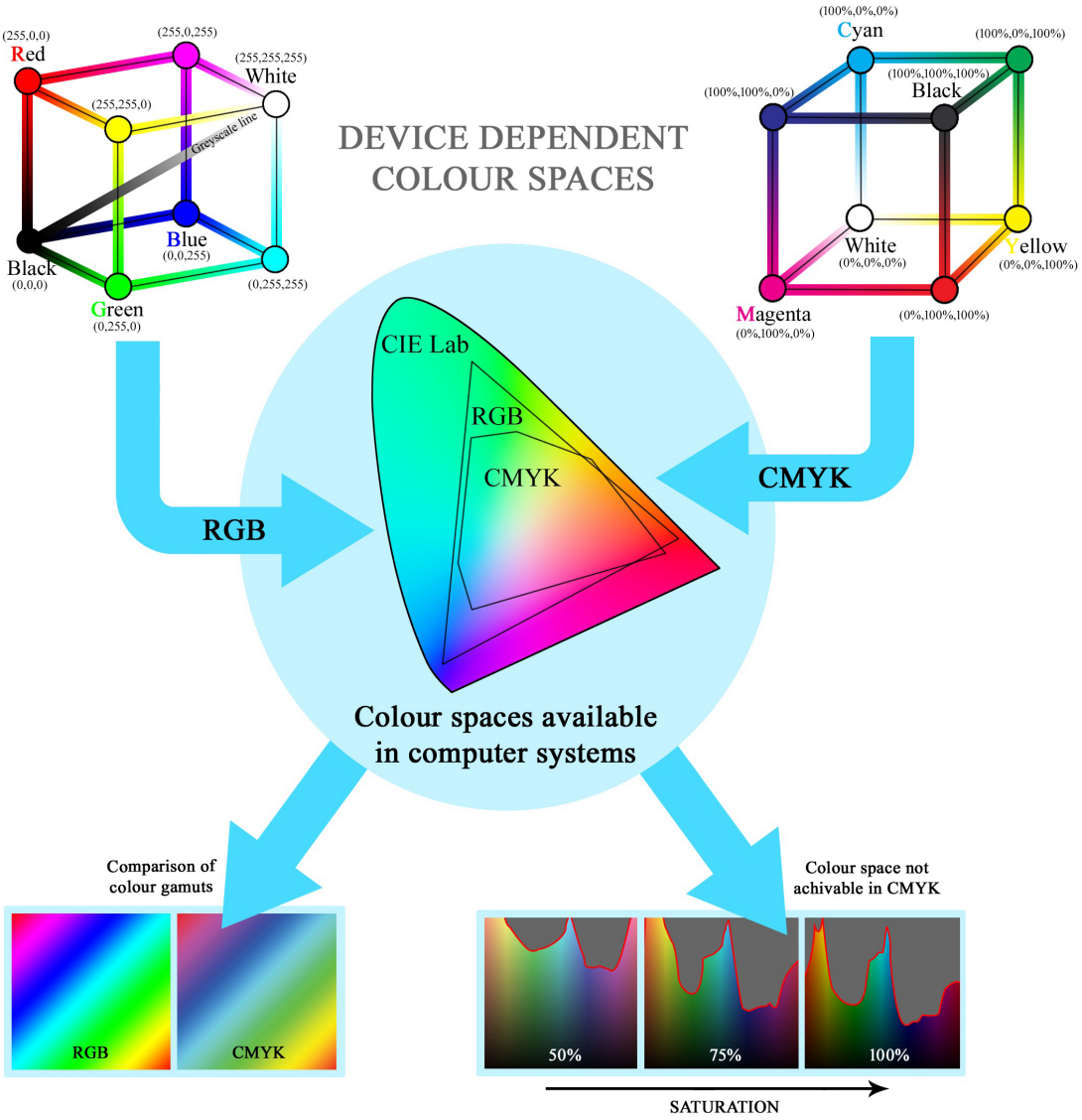

Fig. 1. The most popular colour space models and their advantages and disadvantages

outer compartments over a liquid volume present in the hydraulic mixer (HM). These changes result in adequate liquid flows and liquid height changes in outer (H) and inner (h) compartments. The maximum set pressure in the inner compartment is denoted as P_1 and in outer compartment as P_2. The inner diameter of inner compartment (d_{in}) was equal to 90 mm with wall thickness of 5 mm, while the inner diameter of outer compartment was equal to 190 mm and height of clearance was equal to 40 mm. The distance between bottom and upper dishes was equal to 650 mm. The characteristic time-steps of hydraulic mixing in HM are presented in Fig. 3. More details regarding the hydraulic mixer have been published elsewhere (Mitkowski et al., 2016).

All the experimental measurements were digitally recorded using the Canon Legria HFR88 as mp4 format movies. Bosch GCL 2-15 Professional Digital Laser Level and Bosch Laser Rangefinder were used to ensure repeatable camera settings, known hereafter as field calibration.

The experimental set-up was calibrated in order to unify the measurements in individual cycles and to develop a universal computer analysis method. The idea was to obtain data in the form of movies recorded with the same external factors. This was carried out in order to reduce the minimum number of parameters necessary for input by the user in the created application for image processing.

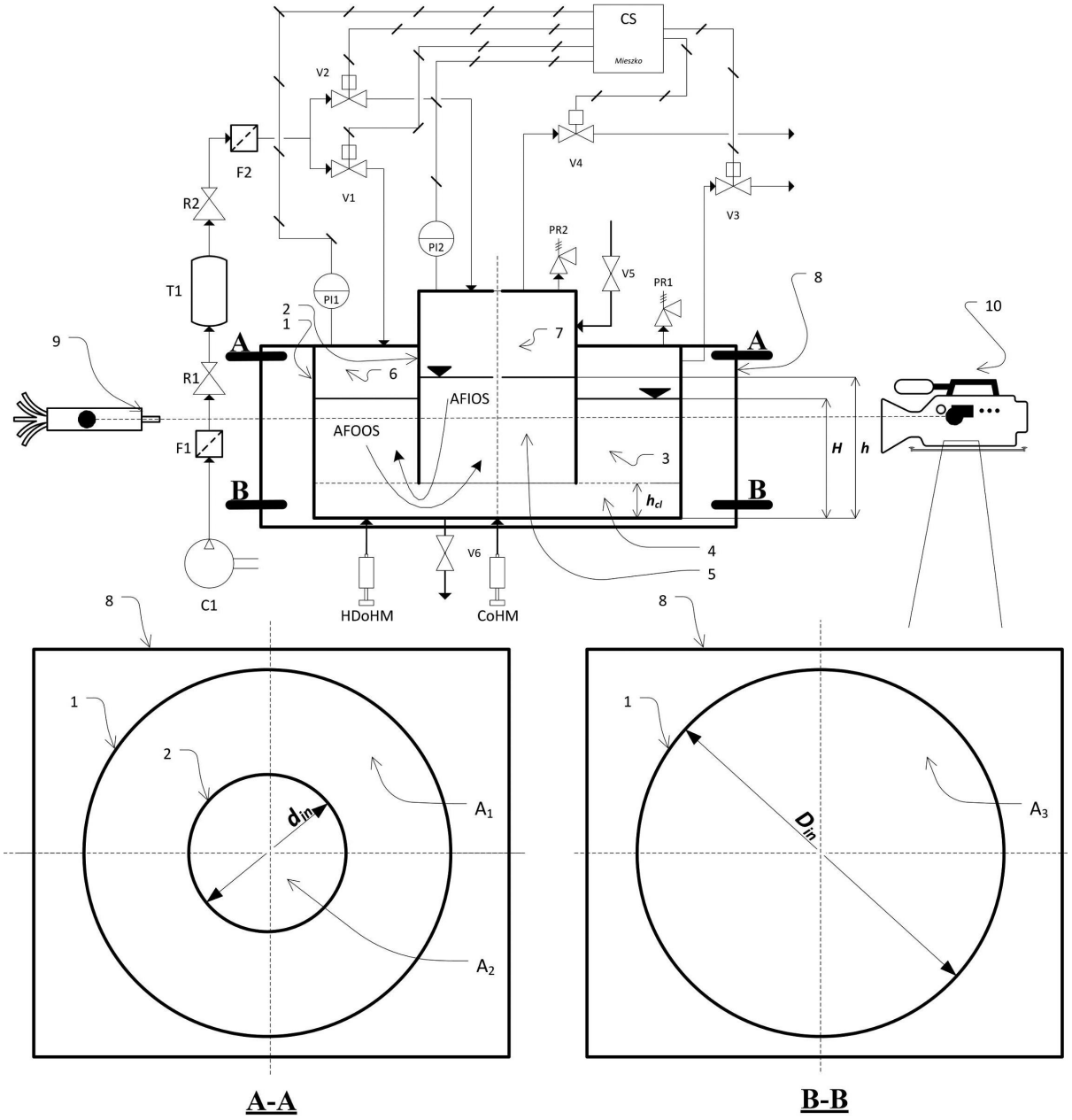

Fig. 2. Hydraulic mixer configuration. Scheme of experimental set-up and camera configuration; C1 – compressor; F1, F2 – air filter; T1 – gas reservoir (27.2 dm^3); R1, R2 – pressure reducing valves; V1 – air inlet valve to outer compartment; V2 – air inlet to inner compartment; V3 – air outlet valve from outer compartment; V4 – air outlet valve from inner compartment; V5, V6 – communicated valves; PR1 – pressure relieve valve in outer compartment; PR2 – pressure relieve valve in inner compartment; PI1 – pressure meter in outer compartment; PI2 – pressure meter in inner compartment; CS – control system connected with PC; 1 – hydraulic mixer casing; 2 – casing of inner compartment; 3 – liquid volume in outer compartment with liquid height H; 4 – common volume with height h_{cl}; 5 – liquid volume in inner compartment with liquid height h; 6 – gas volume in outer comportment; 7 – gas volume in inner compartment; 8 – thermostatic tank; 9 – laser level; 10 – camera; AFOOS – annular flow out of outer space; AFIOS – annular flow into outer space, CoHM – center place of dye injection, HDoHM – half-distance of dye injection, A_1 – cross section of outer compartment, A_2 – cross section of inner compartment, A_3 – cross section of common volume

Before every experiment, the camera and lighting were organized in the same manner and calibrated. The position of the camera was based on the grid lines displayed on the camera screen. The left vertical line was aligned with the left front corner of the square outer tank with the water. The horizontal lines were set with regular distances on a ruler glued to the external tank of the set-up, at the heights of 20 cm and

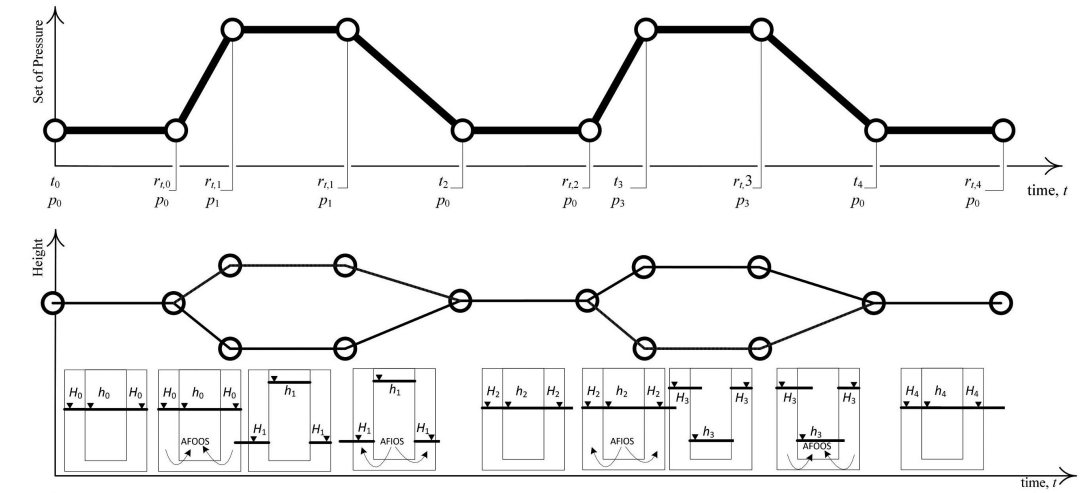

Steps													
Valves	1	2	3	4	5	6	7	8	9	10	11	12	13	14
V1	C	O	C	C	C	C	C	C	C	C	C	C	C	C
V2	C	C	C	C	C	C	C	C	O	C	C	C	C	C
V3	C	C	C	O	C	O	C	O	C	C	C	C	C	C
V4	C	C	C	C	C	O	C	O	C	C	O	C	O	C

Valves position: C – closed, O - open

Fig. 3. Hydraulic mixer configuration. Steps in single cycle in process time scale of hydraulic mixing

40 cm. The height of the camera was aligned to the liquid level using a laser level when the tank was filled in a ratio of $H/D = 1$. The distance of the camera's lens from the wall of the outer tank with water was also determined. It was measured with a laser rangefinder. The distance was 1.110 m. Artificial, constant LED lighting was used to eliminate the influence of differences in natural lighting. The calibration of camera with location of a red laser level indicator are presented schematically in Fig. 2.

In general, intensity of mixing is characterized by Reynolds number, which utilizes velocity and physical properties of a fluid and characteristic dimensions of an object in which the fluid flows. Although in a hydraulic mixer it is impossible to define a single characteristic Reynolds number, it is possible to define characteristic areas A_1, A_2, A_3 (as presented in Fig. 2), and therefore local Reynolds numbers $\mathrm{Re}_{1,i}$, $\mathrm{Re}_{2,i}$, $\mathrm{Re}_{3,i}$, respectively (Eqs. (3)–(5)). All these definitions of local Reynolds numbers use a variation of height in either inner (Δh) or outer (ΔH) compartments and characteristic times $\Delta t_{s,i}$ of steps during a cycle (i.e. $\Delta t_{s,i}$ is equal to either $t_2 - t_1$, $t_4 - t_3$, $t_6 - t_5$ or $t_8 - t_7$; they are graphically presented in Fig. 3

$$A_1 = \frac{\pi}{4}\left(D_{\mathrm{in}}^2 - d_{\mathrm{out}}^2\right) d_{e,1} = \frac{D_{\mathrm{in}}^2 - d_{\mathrm{out}}^2}{D_{\mathrm{in}} + d_{\mathrm{out}}} \quad \rightarrow \quad \mathrm{Re}_{1,i} = \frac{\rho}{\eta}\frac{\Delta H}{\Delta t_{s,i}}\frac{D_{\mathrm{in}}^2 - d_{\mathrm{out}}^2}{D_{\mathrm{in}} + d_{\mathrm{out}}} \tag{5}$$

$$A_2 = \frac{\pi}{4} d_{\mathrm{in}}^2 d_{e,2} = d_{\mathrm{in}} \quad \rightarrow \quad \mathrm{Re}_{2,i} = \frac{\rho}{\eta}\frac{\Delta h}{\Delta t_{s,i}} d_{\mathrm{in}} \tag{6}$$

$$A_3 = \frac{\pi}{4} D_{\mathrm{in}}^2 d_{e,3} = D_{\mathrm{in}} \quad \rightarrow \quad \mathrm{Re}_{3,i} = \frac{\rho}{\eta}\frac{\Delta H}{\Delta t_{s,i}} D_{\mathrm{in}} \tag{7}$$

The flow in volumes characterized with A_1 and A_2 can be easily assumed to be perpendicular to the direction of the liquid flow. However, it is impossible to state, even with great assumption, that the flow would be perpendicular to the surface represented by the area A_3. Nevertheless, that one more characteristic area $A_{h_{cl}}$ restricted by clearance height h_{cl} and the edge of inner compartment (item 2 in Fig. 2) characterized by circumference with its mean diameter $\overline{d_{\mathrm{in}}}$ can be distinguished, therefore leading to the definition of Reynolds number presented in Eq. (6).

$$A_{h_{cl}} = \pi \overline{d_{\mathrm{in}}} h_{cl} d_{e,4} = \frac{2\pi \overline{d_{\mathrm{in}}} h_{cl}}{\pi \overline{d_{\mathrm{in}}} + h_{cl}} \quad \rightarrow \quad \mathrm{Re}_{4,i} = \frac{\rho}{\eta}\frac{\Delta h}{2\Delta t_{s,i}}\frac{\pi d_{\mathrm{in}}^2}{\pi \overline{d_{\mathrm{in}}} + h_{cl}} \tag{8}$$

Due to the operational stepwise variations in liquid heights made by gas pressure changes in compartments, the hydraulic mixing is assumed to be semi-continuous which is characterized by predefined and repetitive

liquid height changes. Note, that gas pressure is causing the fluid movement while mixing is caused by fluid movement from one compartment to another. To describe the hydrodynamics of hydraulic mixing, Mitkowski and co-authors (Mitkowski et al., 2016) proposed a modified Reynolds number for hydraulic mixing $\overline{\mathrm{Re}_{\mathrm{HM}}}$ (Eq. (9). The concept behind $\overline{\mathrm{Re}_{\mathrm{HM}}}$ is that each step is characterized by the averaged linear velocity $w_{s,i}$ of liquid (Eq. (11)) which is counted as change in heights of liquid in inner and outer compartments (Eq. (12)).

$$\overline{\mathrm{Re}_{\mathrm{HM}}} = \sum_{\substack{i=1\\j=1}}^{n} \mathrm{Re}_{\mathrm{HM},i,j} \frac{t_{\mathrm{cycle},j}}{t_p} \tag{9}$$

$$\mathrm{Re}_{\mathrm{HM},i} = \frac{w_{s,i} d_e \rho}{\eta} \tag{10}$$

where:

$$w_{s,i} = \frac{h_{T,s,i}}{t_{s,i}} \tag{11}$$

$$h_{T,s,i} = \left|H_{\mathrm{in},s,i} - H_{f,s,i}\right| + \left|h_{\mathrm{in},s,i} - h_{f,s,i}\right| \tag{12}$$

$$d_e = \frac{4\overline{d_{\mathrm{in}}} h_{cl}}{D_{\mathrm{in}} + d_{\mathrm{out}} + d_{\mathrm{in}}} \tag{13}$$

where: $\mathrm{Re}_{\mathrm{HM}i,j}$ is the characteristic cycle Reynolds number in i-th step of the j-th cycle, $t_{\mathrm{cycle},j}$ is the duration time of the j-th step, t_p is the hydraulic mixing process time, $t_{s,i}$ is the characteristic time of step i which is equivalent to the time in which the heights of liquid-gas interfaces have changed between its maximum and minimum values, $H_{\mathrm{in}s,i}$ is the initial height of liquid in outer compartment in step i (m), $H_{f,s,i}$ is the final height of liquid in outer compartment in step i (m), $h_{f,s,i}$ is the final height of liquid in inner compartment in step i (m), $h_{\mathrm{in}s,i}$ is an initial height of liquid in inner compartment in step i (m), d_{in} is the inner diameter of inner compartment, d_{out} is the outer diameter of inner compartment and h_{cl} is the height of clearance (m).

Incorporating Eqs. (7) and (9) into (5) under assumption that $t_{\mathrm{cycle},j}$ is equal to $t_{s,i}$ allows to define the averaged characteristic Reynolds number as follows:

$$\overline{\mathrm{Re}_{\mathrm{HM}}} = \frac{\rho}{\eta} \frac{4\overline{d_{\mathrm{in}}} h_{cl}}{D_{\mathrm{in}} + d_{\mathrm{out}} + d_{\mathrm{in}}} \frac{1}{t_p} \sum_{i=1}^{n} \left[\left|H_{\mathrm{in},s,i} - H_{f,s,i}\right| + \left|h_{\mathrm{in},s,i} - h_{f,s,i}\right|\right] \tag{14}$$

3. FRAMEWORK, METHODS, AND TOOLS

In general, conducting the experiments required careful planning and establishing the framework which would lead to the defined goal. The framework consists of three main stages: experiment preparation, experimental procedure, and analysis of experimental results (see Fig. 4). The objective and goals of the experiment (or set of experiments) are defined in the first step of framework (1F). In the second step (2F), the hydraulic mixing experiment is performed with appropriate recording. After concluding the experiment, the post-experimental procedure consisting of cleaning, maintenance activities and image analysis is carried out. The image analysis follows the methodology of Computer-aided Image Analysis for Hydraulic Mixing which is presented in detail in the next chapter. The results of image analysis along with other data (such as recording of pressure indicators) are analysed in step 3F.

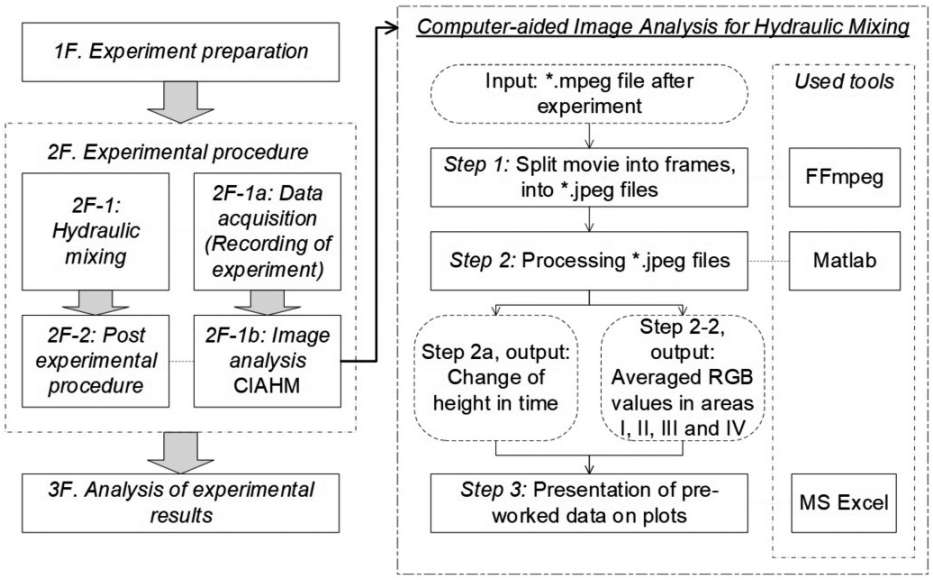

Fig. 4. General framework and methodology of Computer-aided Image Analysis for Hydraulic Mixing

3.1. Methodology of computer image analysis for hydraulic mixing

The essential part of experimental framework of the hydraulic mixing experiment is the methodology of Computer-aided Image Analysis for Hydraulic Mixing (CIA4HM) presented in Fig. 4. During the experiment, a movie is recorded and usually a single experiment consists of a single movie (format: mp4, frame rate: 59.94 frames/second, frame width: 1920 px, frame height: 1080 px) but this is not always the case. The obtained movie is postprocessed off-line according to the CIA4HM.

The first step of CIA4HM analysis is to split the recorded movie into single frames which are saved in the jpg file format (step 1). That operation was carried out using FFmpeg (Bellard, 2015), a command line operated software, because of very robust process which lasted for 30 minutes per approx. 5 minutes of the movie using a regular PC (processor: Intel®Core™i5-4460 CPU @ 3.20GHz, RAM: 8.00 GB). The recording was split with an accuracy of one frame. For this purpose, it was necessary to enter such parameters as: file name, frame numbering after division, file format. All jpg files formed a set of pictures (a 30 minute movie resulted in 107 892 jpeg files). The set of image files is an input for the next step and is processed using the MATLAB environment, i.e. step 2 (see Fig. 4). Processing jpeg files. In step 2, each saved frame gained a unique identifier, which allowed to locate the selected frame(s) on the local disk of the computer. The main goal of the prepared code in the Matlab environment was to analyse each jpeg file in order to obtain data for each specific time point corresponding to the result of hydraulic mixing. Two possibilities of data analysis were programmed: a change of height over time and a change of values of RGB components in defined areas over time. The user can choose the type of analysis depending on the parameters of the process which need to be examined. In this study, both sets of data were obtained and collected for analysis in step 3F. Both options are described in detail further in this chapter. The results of the coded scripts in Matlab are (1) liquid height in the outer and inner tank in the function of time and (2) changes in concentration of subsequent frames and cycles. The results of step 2 are then processed in Microsoft Excel.

3.2. Change of height over time

The change of height in each movie's frame is obtained during step 2a of CIA4HM. The changes of liquid heights are important for analysis of mixing efficiency. Therefore, there is a need for tracking it during the process time. The exact determination of height changes in HM is necessary for further analysis of

the process hydrodynamics, especially for calculation of modified Reynolds number, i.e. $\overline{\mathrm{Re}_{\mathrm{HM}}}$. In general, the level of liquid, called the liquid height, is determined by reading the value from a ruler located on the thermostatic tank (number 8 in Fig. 2) filled with water. The algorithm processes each frame and identifies the interface location based on the RGB data at a line predefined by the user (see the red line in Fig. 5a). The line was defined in the outer compartment based on observation and is close to the inner wall where the background is lighter to ease the search for an interface location. The code contains the function finding the greatest value of the difference in RBG components along the defined horizontal lines. The line is horizontal in the picture, while in reality this line is vertical. The largest variation is noticeable in the interfacial space. That was demonstrated with a snapshot from the Pixel Region tool in Matlab (see Fig. 5a). Determination of the liquid level allows to track the whole process and easily identify the level of instability within the mixing system.

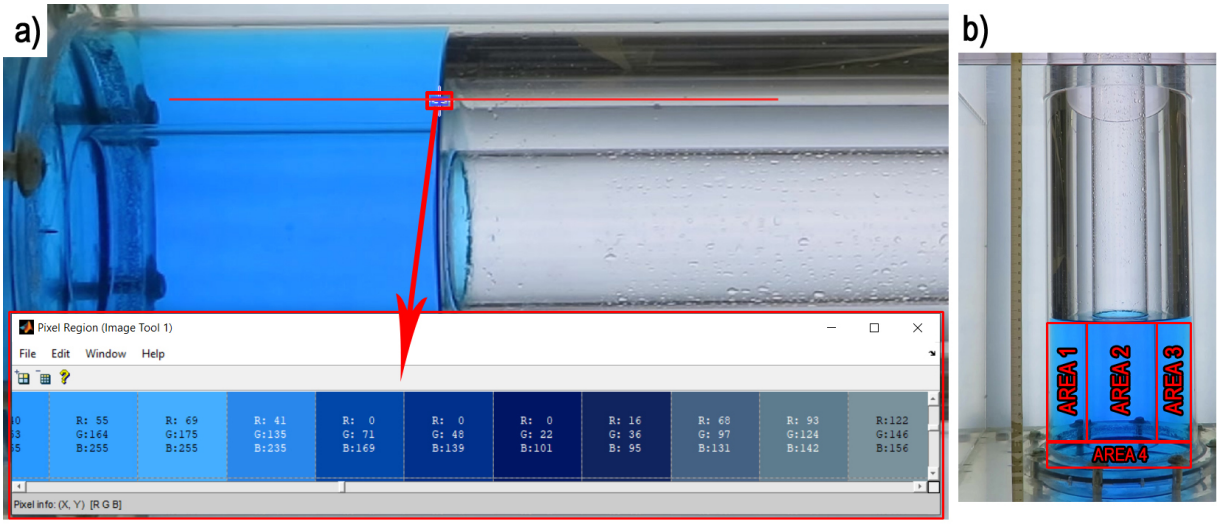

Fig. 5. Image analysis aspects in hydraulic mixer. a) The rule for determining the height of liquid in the external cylinder of the tank visualized with the Pixel Region tool in Matlab. b) Specific areas of colour analysis in hydraulic mixer (HM). Dimensions of AREA1 and AREA3 is equal to 32×123 mm (92×351 px) and AREA2 has 68×123 mm (194 × 351 px)

3.3. RGB values in predefined areas

The RGB values are obtained in Step 2b of CIA4HM. In general, each frame of a movie has to be analysed in order to retrieve the characteristic data of RGB. In order to obtain the performance of the hydraulic mixing, colour changes in the same part of each cycle are analysed. It is done at the end of each cycle, more precisely at t_9 (see the plot in Fig. 3), which also corresponds to the 14^{th} step in the valve configuration also presented in the table in Fig. 3. The entire single frame showing the liquid in HM was divided into four areas due to the specificity of the HM. The result of this part of image analysis is a table with a complete list of R, G and B values in each pixel of the areas.

3.4. Calculation of apparent concentration of dye

Concentration distribution is the main parameter which characterizes the homogeneity of the mixing process. In this study, the concept of apparent concentration of dye calculated on the basis of obtained RGB values in selected areas was utilized in step 3F. The apparent concentration was calculated based on the colour difference occurring in the mixer.

B-value of the RGB colour space model, namely blue, was used in the calculations because of the highest sensitivity of that component to variations in the range of experimental concentrations. This reduced the calculation error and allowed to present the actual concentrations according to Eq. (15).

$$C = \frac{\mathrm{B}_j - \mathrm{B}_{\mathrm{in}}}{\mathrm{B}_f - \mathrm{B}_{\mathrm{in}}} \cdot 100\% \tag{15}$$

The apparent concentration C was calculated for each of the three areas independently in order to precisely compare the degree of mixing in compartments but with the same values of B_f and B_{in} in all analysed areas for specific experiment. Note, that B_{in} was taken as the reference just before starting the experiment. Area 4 was not included in the analysis of the results due to high colour disruptions related to the bottom construction and almost constant concentration since the beginning of experiment.

Charts of dye concentration in the function of hydraulic mixing process cycles are presented further. The obtained RGB values were presented in the form of colour in a defined cell of spreadsheets in MS Excel with a formula written in Visual Basic for Applications module. Input values for the function are the averaged values of the RGB components of each pixel in any area.

4. APPLICATION OF FRAMEWORK AND CIA4HM METHODOLOGY

4.1. Experiment preparation (step 1F)

The data presented in this chapter were obtained in the hydraulic mixer, which was described in detail in (Mitkowski et al., 2016). In this case study, a set of six experiments listed in Table 1 was investigated. The objective was to investigate the influence of a set of pressures P_1 and P_2 (see Table 1, part A) on the mixing performance. The mixer was filled with deionized water at a ratio of $H/D = 1$. The next step was to set specific pressure values in the control system CS (see CS in Fig. 2). The dye (bromothymol blue 3 w%, 3 ml) was centrically injected (CoHM, Fig. 2) with an automatic syringe into the hydraulic mixer with a flowrate equal to 0.12 ml/s. Then, hydraulic mixing was initiated.

4.2. Hydraulic mixing (step 2F-1)

The completeness of mixing at the end of the experiment was assessed visually by the researcher, firstly during the experiment and secondly during the video analysis. The assessment considered the places of incomplete mixing, which sometimes might last for a long time (as presented in Fig. 11 which it will be discussed later on). This results from the fact that these areas might sometimes have not been detected further in a generalized computer analysis. The problem relates to the outer areas of the outside cylinder of the mixer.

4.3. Recording of experiment (step 2F-1a)

An individual measurement was digitally recorded during the experiment using a camera (step 2F-1). All movies were recorded in a 1920 × 1080 px resolution with a frequency of 59.94 fps. The recording always started before the mixing process, usually during dye addition and ended after achieving complete mixing in all areas. Therefore, the total number of analysed frames is always higher than those needed for computations. A detailed list of analysed frames and related times in each movie are listed in Table 1 (part B).

Table 1. Summary of analysed experiments

Experiment number	E1	E2	E3	E4	E5	E6
A. Defined process parameters*						
P_1 [hPa]	200	200	170	170	120	120
P_2[hPa]	150	100	100	50	30	20
B. Recording parameters						
Number of frames in recorded movie	45 134	68 131	57 540	117 258	59 374	59 334
Time of experiment [s]	753	1 137	960	1 956	991	990
Number of frames in final analysis	43 562	66 388	56 243	115 045	57 126	58 535
Time of mixing [s]	727	1 108	938	1 919	953	977
C. Process characteristics obtained from CIA4HM						
Duration of measurement [s]	727	1 137	938	1 956	991	990
min h [cm]	9.66	12.80	14.23	14.78	17.97	16.93
Standard deviation min h [cm]	0.16	0.06	0.08	0.13	0.07	0.06
max h [cm]	23.06	23.25	23.20	22.73	22.19	22.18
Standard deviation max h [cm]	0.07	0.05	0.07	0.02	0.06	0.04
Δh [cm]	13.40	10.45	8.96	7.95	4.21	5.26
min H [cm]	16.40	17.05	17.81	17.27	18.07	18.07
Standard deviation min H [cm]	0.04	0.03	0.04	0.01	0.03	0.02
max H [cm]	23.71	22.76	22.70	21.61	20.44	20.94
Standard deviation max H [cm]	0.09	0.03	0.04	0.07	0.04	0.03
ΔH [cm]	7.31	5.71	4.89	4.34	2.37	2.87
$\Delta h + \Delta H$ [cm]	20.71	16.16	13.86	12.29	6.59	8.13
Number of cycles	21	34	29	61	25	25
Average cycle time [s]	34.61	32.58	32.36	31.46	38.12	39.06
Standard deviation of average cycle time [s]	0.83	1.32	0.50	1.14	0.22	0.13
max $\overline{\mathrm{Re}_{\mathrm{HM}}}$	3.4E+07	2.6E+07	2.2E+07	2.6E+07	2.7E+07	3.0E+07

*Clearance height (h_{cl}) for all experiments was equal to 40 mm.

4.4. Image analysis (step 2F-1b)

Each of the recorded movies was processed according to the procedure described in Section 3. The first important output from the CIAHM is a change of height in time (step 2a), which allows to identify characteristic process steps in time (for example beginning of cycle), average heights in inner (h) and outer (H) compartments and evolution of modified Reynolds number of hydraulic mixing (denoted on plots as $\mathrm{Re}_{\mathrm{HM}}$). The exemplary visualisation of the obtained results of height change are presented in Fig. 6. The second output (step 2-2) consists of RGB data which are discussed in detail in Section 4.5.2.

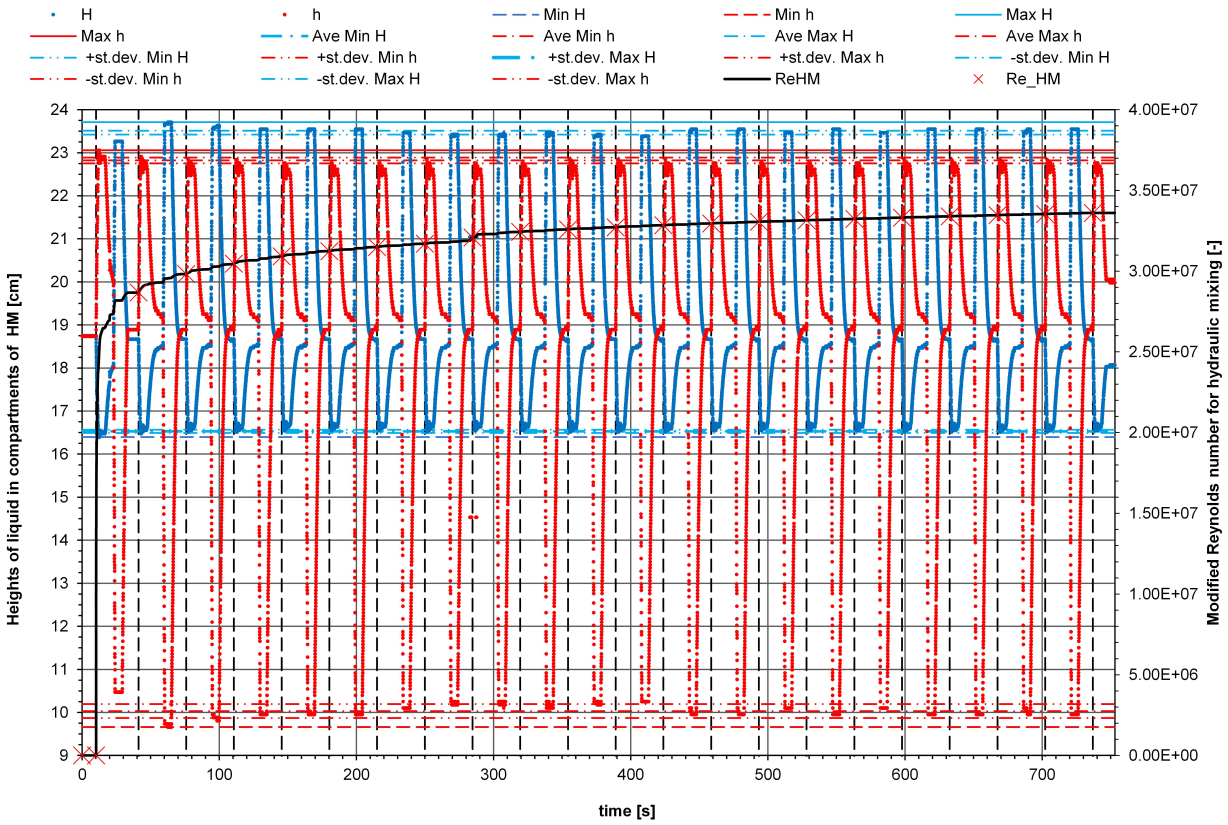

Fig. 6. Visualization of all process parameters for experiment E1 obtained based on image analysis

4.5. Analysis of experimental results (step 3F)

4.5.1. Analysis of height changes during mixing

One of the CIA4HM outputs is data describing the change of liquid heights in the outer and inner compartments along with values of modified Reynolds number. The summary of experimental data related to liquid level is listed in Table 1 (part C). It should be emphasized that the time between each point is equal to 0.017 seconds.

Variation of liquid height at maximum and minimum inclines does not exceed 2%, which is not more than 2 mm in absolute terms. This confirms the good repeatability of process steps and accuracy of the proposed method. In general, implication of higher pressures (i.e. P_1 and P_2) results in an increase of the change in liquid levels in the inner compartment (Δh) and outer compartment (ΔH). The highest change of liquid levels ($\Delta h + \Delta H$) in E1 results in the highest values of modified Reynolds number, lowest number of cycles needed to achieve good mixing, which also results in the shortest time of mixing. Proper mixing is defined here by achievement of 100% of dye concentration. The maximum value of modified Reynolds number for hydraulic mixing reported in Table 1 ($\max \overline{\mathrm{Re}_{\mathrm{HM}}}$) is defined as the value of $\overline{\mathrm{Re}_{\mathrm{HM}}}$ at which proper mixing was achieved. At first glance it seems surprising that E5 and E6, with the lowest values of applied pressures, gave such good results. Both E5 and E6 needed 25 cycles to reach proper mixing, while others (except E1) needed at least four more cycles. These results can be related to the longer time of cycle which allows higher impact of inertia on hydraulic mixing. This observation is confirmed by the fact that high values of modified Reynolds number were reached (see Table 1, part C). However, based on the presented results, it is impossible to state which value of Reynolds number is limiting the mixing.

4.5.2. Changes in apparent concentration in subsequent cycles

The second output from the CIA4HM methodology is representing the average RGB values in the preselected areas of the hydraulic mixer. Figures 7–12 show the results for all six experiments as plots of apparent dye concentrations in three areas in the function of cycle number. Additionally, that area is disturbed by a large influence of the bolts at the bottom of the mixer which reflect light. It has to be highlighted that background colour in Figures 7–12 represents the maximum RGB colour while numbers provide apparent concentration of dye, which is an averaged value within the whole area. Each figure presenting the concentration change is enriched with a plot showing the modified Reynolds number for hydraulic mixing at the end of specific cycle.

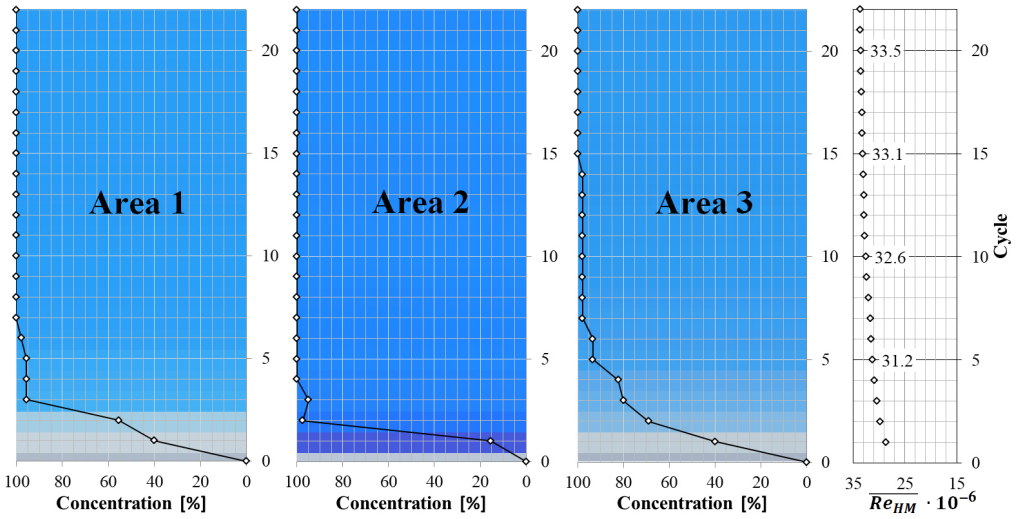

Fig. 7. Concentration dependence on hydraulic mixing cycle in areas of experiment 1

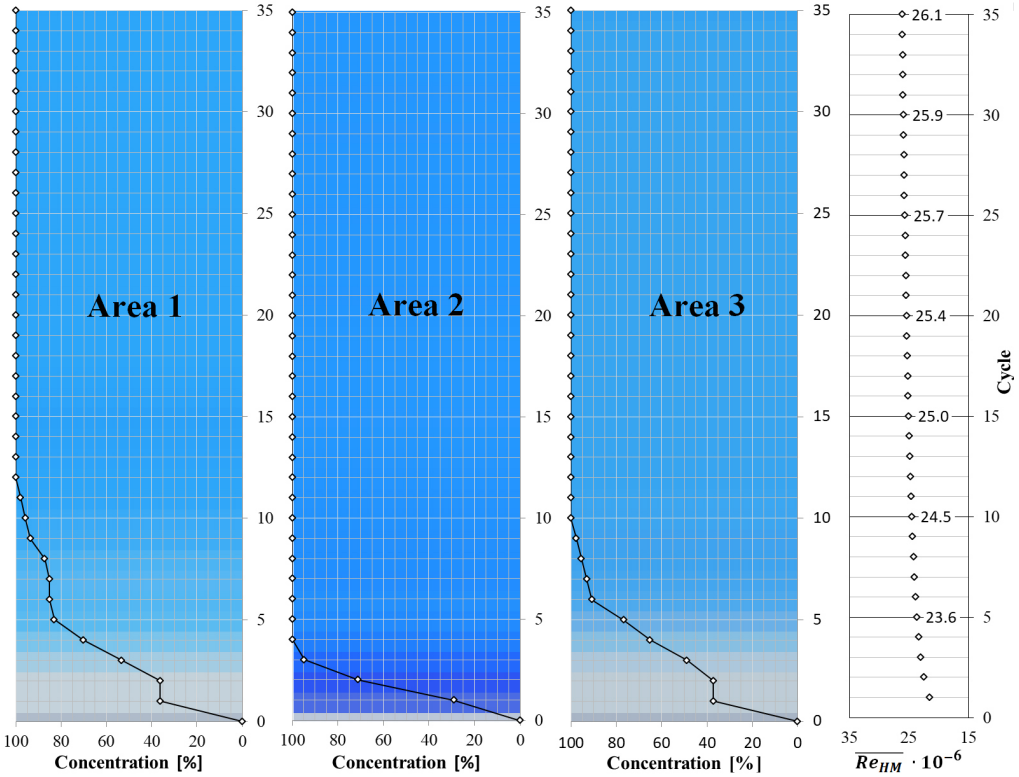

Fig. 8. Concentration dependence on hydraulic mixing cycle for 3 areas of experiment 2

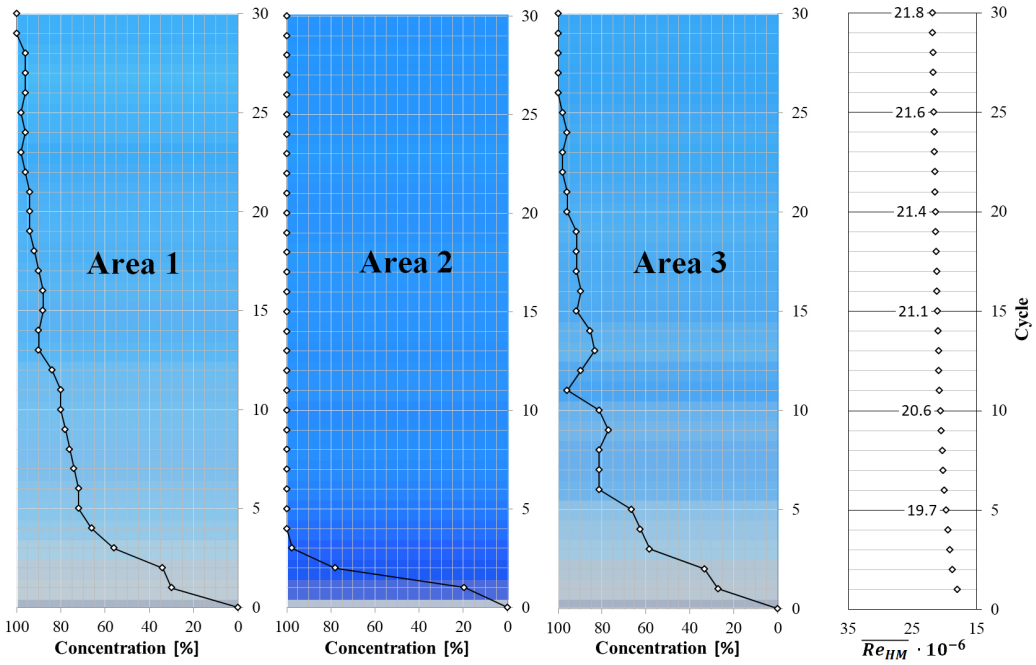

Fig. 9. Concentration dependence on hydraulic mixing cycle for 3 areas of experiment 3

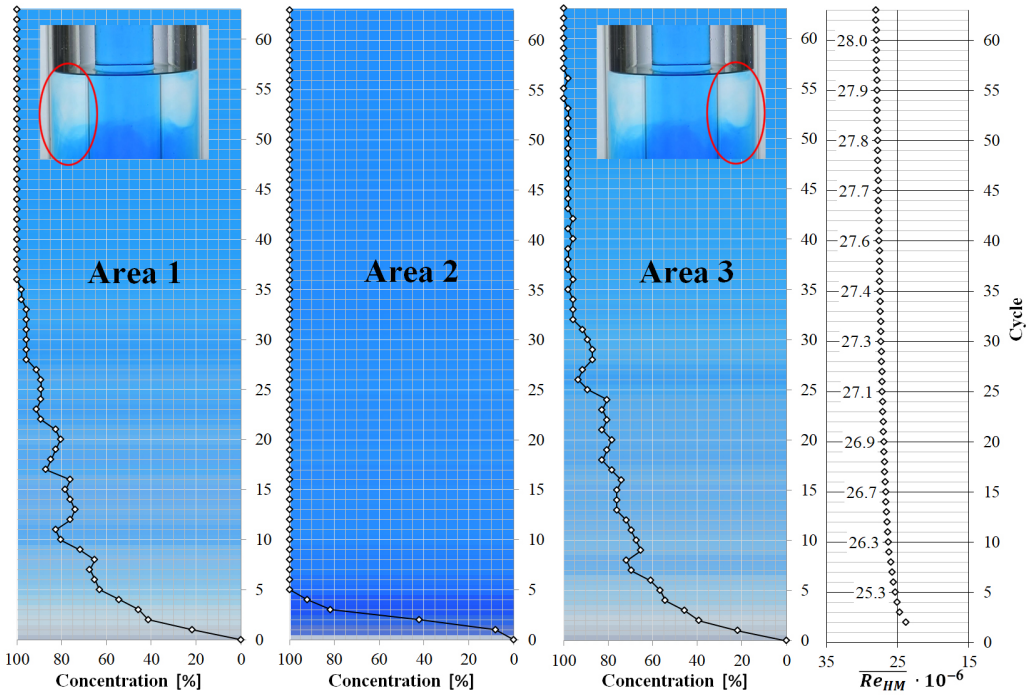

Fig. 10. Concentration dependence on hydraulic mixing cycle for 3 areas of experiment 4. Inserted pictures in areas 1 and 3 are taken in cycle 53

At first glance there are discrepancies in concentrations between areas 1 and 3 although they represent the same compartment. It is especially evident when comparing results for experiments E1, E3, E4 and E6. The authors postulate that these discrepancies show some unpredictability and inherent variation of hydraulic mixing, rather than influence of the gas inlet and outlet to outer compartment. It is based on the fact that the mixer was levelled and kept in the same position for all experiments, and the achievement of higher concentration was sometimes present in the area 1 (i.e. E1 and E4) while at other times in area 3 (i.e. E3 and E6).

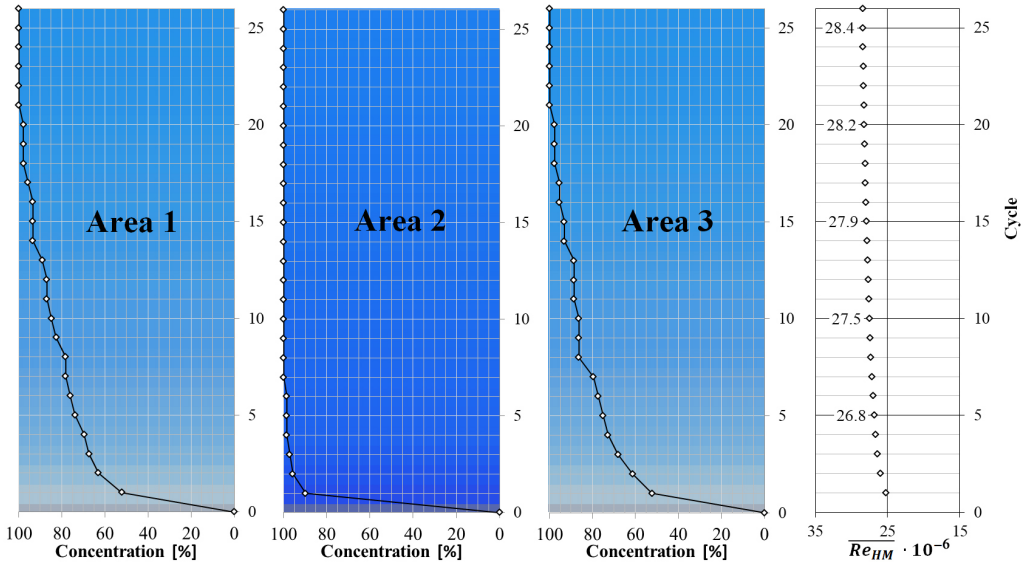

Fig. 11. Concentration dependence on hydraulic mixing cycle for 3 areas of experiment 5

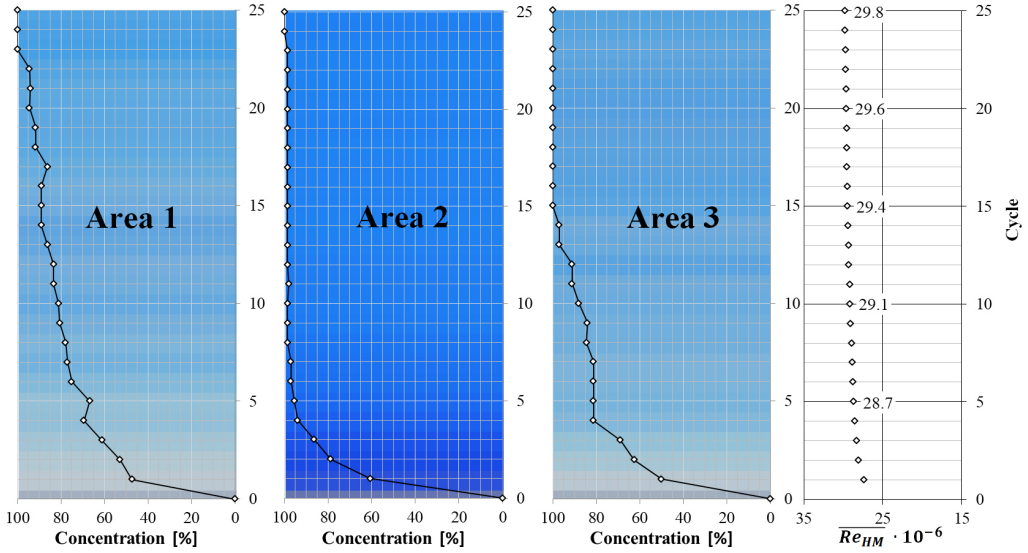

Fig. 12. Concentration dependence on hydraulic mixing cycle for 3 areas of experiment 6

In experiment E1 the proper mixing defined by achievement of 100% of dye concentration in defined areas was reached at a different time, i.e. in area 2 after the 4th cycle, in area 1 after the 7th cycle and in area 3 after the 14th cycle. It is not surprising that dye distribution in area 2 was the fastest since it reflects the inner compartment, which is smaller in volume than the outer one. The change in height was almost double in comparison to the outer compartment (Δh = 13.4 cm vs. ΔH = 7.3 cm) and local Reynolds numbers for the inner compartment were generally higher than those for the outer compartment (which has been discussed in more detail elsewhere (Mitkowski et al., 2016)). The discrepancies between areas 1 and 3 are surprising since both represent the outer compartment which is symmetrical. The authors relate that phenomenon to the fact that local Reynolds numbers calculated for the outer compartment are mainly within the laminar regime except time step between points t_5 and t_6 (for values see Table 2, while for meaning of t_5 and t_6 see Fig. 3) and strike phenomenon was already discussed in (Mitkowski et al., 2016). Similar conclusions can be drawn from other experiments (E2-E6) based on the presented Figures 7–12. In general, 100% of dye concentration was obtained at first in the inner compartment (area 2) and then in the outer compartment (areas 1 and 3). It is usually reached within four cycles, except for E5 and E6 where

it is obtained after 7 and 24 cycles. Achievement of specific concentration within the outer compartment (i.e. areas 1 and 3) is slower and it is asymmetric. Proper mixing in all presented experiments was obtained within 21 and 61 which corresponds to the range of $2.1 \cdot 10^7$ (E4) and $3.4 \cdot 10^7$ (E1). These results also suggest that there is higher axial mixing than radial mixing in the outer compartment. Moreover, mixing in the outer compartment has a diffusive character in radial direction. That observation is supported by the fact that flow in outer compartment has a laminar characteristic (see Table 2 and Mitkowski et al., 2016).

Table 2. Values of local Reynolds numbers

	$Re_{1,i}$	$Re_{2,i}$	$Re_{4,i}$	$Re_{1,i}$	$Re_{2,i}$	$Re_{4,i}$	$Re_{1,i}$	$Re_{2,i}$	$Re_{4,i}$	$Re_{1,i}$	$Re_{2,i}$	$Re_{4,i}$
Experiment No.	$\Delta t_{s,i} = t_2 - t_1$			$\Delta t_{s,i} = t_4 - t_3$			$\Delta t_{s,i} = t_6 - t_5$			$\Delta t_{s,i} = t_8 - t_7$		
1	1187	*2295*	1012	263	509	224	**3606**	**6974**	**3075**	832	1609	709
2	1191	*2303*	1015	276	534	236	*2516*	**4865**	2145	748	1447	638
3	1052	2035	897	290	560	247	**3015**	**5831**	*2571*	651	1259	555
4	1188	*2297*	1013	250	483	213	**3282**	**6347**	*2798*	654	1264	557
5	1135	2195	968	178	344	152	1669	**3227**	1423	471	911	402
6	942	1822	803	187	362	160	1804	**3489**	1539	502	970	428

Bold font – turbulent flow, italic font – transient flow, underlined – laminar flow

An increase in the sum of level differences ($\Delta h + \Delta H$, see Table 1) causes the fastest (i.e. smaller number of cycles) reaching of 100% of dye concentration, although visual researcher-based assessment shows that more cycles are needed to achieve completeness of mixing. Therefore, it shows that the proposed methodology has deficiencies in that area and needs further improvements. Future development can be oriented on redefining areas of colour analysis, investigating other colour model components and subtracting the background colour.

5. CONCLUSIONS

This contribution presented the general methodology of the CIA4HM framework which consisted of three main steps and utilized three computer-aided tools. With use of CIA4HM, it is possible to obtain data which represent the change of heights in time and averaged RGB values in preselected areas in the hydraulic mixer. The framework was supported with the application to six experiments.

The presented results clearly show that the change of liquid levels in the outer and inner compartments along with cycle time plays the key role in hydraulic mixing. Increase of change of liquid levels and decrease of cycle time decrease the mixing time. However, experiments E5 and E6 show that a significant decrease in the change of liquid heights with increase of cycle time resulted in results similar to those with higher change of liquid heights but with smaller time. Therefore, there is room for future optimization of the influence of these parameters on hydraulic mixing efficiency.

The concept of using modified Reynolds number for hydraulic mixing previously presented by Mitkowski (2016) was used. There is no clear relation between its value and achievement of proper mixing. Based on the obtained results, it can be stated that proper mixing is obtained when the modified Reynolds number reaches values of $2.6–3.4 \cdot 10^7$. However, that range can be used as the first approximation when proper mixing can be achieved in the process of hydraulic mixing.

The presented CIA4HM methodology significantly increases data processing speed in comparison to the method for image analysis presented and used previously in (Mitkowski et al., 2016). Obtaining results from a single movie for one experiment lasted approx. 30 minutes now take up to 60 minutes and mainly depend on the computing power of the computer. Previously, manual processing of the results was case sensitive and lasted up to several days. Moreover, the CIA4HM methodology has potential to be applied to similar processes and/or for other image-based process analysis, although it needs improvement.

The assessment of the degree of mixing using the RGB colour model (presented in Section 4.5.2) may be imprecise due to the dependence of the formula describing hue on the maximum R, G or B values. The values at the limit of the maxima have quite significant hue deviations. The method of colour analysis requires further development. For that purpose, it is planned to develop a calibration curve for various colours, exclusion of the background image from the analysis and to select an alternative colour model component, which will enable unambiguous tracking of the concentration change.

The average value of colour in the areas does not allow to evaluate mixing very accurately. The presented results of colour analysis are generalized for a specific area. Despite the stabilized average value, incomplete mixing was observed in the outer compartment represented by areas 1 and 2. For that reason, the hydraulic mixing process was carried out until complete mixing was achieved based on a visual evaluation of researchers. The colour in each pixel of the obtained image should be analysed to achieve a more accurate result. In addition, it is necessary to determine the variability of concentration results, calculated in relation to the average value. The relative standard deviation may be the measure of variability.

This study clearly shows the need for further development of methodology of computer-aided image analysis for hydraulic mixing, which would allow to better understand this process, its optimization and applicability in industrial practice.

This research was supported by the Polish Ministry of Education and Science subsidy for Poznan University of Technology.

SYMBOLS

B_f	value of the B component in final cycle
B_{in}	value of the B component in initial cycle
B_j	value of the B component in j cycle
CMYK	Cyan Magenta Yellow Key colour model
C	concentration in tank in cycle j, %
D_{in}	inner diameter of outer compartment of the tank, m
d_e	equivalent diameter, m
d_{in}	inner diameter of the inner compartment, m
d_{out}	outer diameter of the inner compartment, m
H	height of the tank, m
h_{cl}	height of clearance, height of gap, m
$h_{f,s,i}$	final height of liquid in inner compartment in step i, m
$H_{f,s,i}$	final height of liquid in outer compartment in step i, m
$h_{in\,s,i}$	initial height of liquid in inner compartment in step i, m
$H_{in\,s,i}$	initial height of liquid in outer compartment in step i, m
$h_{T\,s,i}$	total height which liquid-gas interfacial surfaces travelled over the total mixing time, m
HM	hydraulic mixer

ICC	International Colour Consortium
P_1	pressure in outer compartment, hPa
P_2	pressure in inner compartment, hPa
$\mathrm{Re}_{\mathrm{HM}i,j}$	characteristic stage Reynolds number in step i
$\overline{\mathrm{Re}_{\mathrm{HM}}}$	modified Reynolds number for hydraulic mixing
RGB	Red Green Blue colour model
S	saturation
$t_{\mathrm{cycle},i}$	time of i cycle, s
t_p	hydraulic mixing process time, s
$t_{s,i}$	characteristic time of a step during stage i, s
$w_{s,i}$	average step linear velocity in i step, m/s

Greek symbols

η	dynamic viscosity, Pa·s
ρ	density, kg/m^3

REFERENCES

Afshari-Jouybari H., Farahnaky A., 2011. Evaluation of Photoshop software potential for food colorimetry. *J. Food Eng.*, 106, 170–175. DOI: 10.1016/j.jfoodeng.2011.02.034.

Bellard F., 2015. FFmpeg. A complete, cross-platform solution to record, convert and stream audio and video. Available at: http://ffmpeg.org/.

Bishop M.D., 1992. Converter to convert a computer graphics signal to an interlaced video signal. US5455628A.

Bratkova M., Boulos S., Shirley P., 2009. oRGB: A practical opponent color space for computer graphics. *IEEE Comput. Graphics Appl.*, 29, 42–55. DOI: 10.1109/mcg.2009.13.

Cabaret F., Bonnot S., Fradette L., Tanguy P.A., 2007. Mixing time analysis using colorimetric methods and image processing. *Ind. Eng. Chem. Res.*, 2007, 46, 14, 5032–5042. DOI: 10.1021/ie0613265.

Eliceiri K.W., Rueden C., 2005. Invited review tools for visualizing multidimensional images from living specimens. *Photochem. Photobiol.*, 81, 1116-1122. DOI: 10.1562/2004-11-22-IR-377.

Ferreira T., Rasband W., 2012. *ImageJ User Guide. IJ 1.46r*. Available at: https://imagej.nih.gov/ij/docs/guide/user-guide.pdf.

Galer M., Horvat L., 2003. *Digital imaging: Essential skills*. 3rd edition. *Focal Press*. DOI: 10.4324/9780080472515.

Ghanem A., Lemenand T., Della Valle D., Peerhossaini H., 2014. Static mixers: Mechanisms, applications, and characterization methods – A review. *Chem. Eng. Res. Des.*, 92, 205–228. DOI: 10.1016/j.cherd.2013.07.013.

Hardt, S., Schönfeld, F., 2003. Laminar mixing in different interdigital micromixers: II. Numerical simulations. *AIChE J.*, 49, 578–584. DOI: 10.1002/aic.690490305.

Jankowski M., 2006. *Elementy grafiki komputerowej*. WNT, Warszawa.

McAndrew A., 2004. An introduction to digital image processing with Matlab. Notes for SCM2511 Image Processing 1. Available at: https://www.hlevkin.com/hlevkin/49octaveImageProc/Books/McAbdrew-An%20Introduction%20to%20Digital%20Image%20Processing%20with%20Matlab.pdf.

Mitkowski P.T., Adamski M., Szaferski W., 2016. Experimental set-up of motionless hydraulic mixer and analysis of hydraulic mixing. *Chem. Eng. J.* 288, 618–637. DOI: 10.1016/j.cej.2015.12.012.

Molenda J., Wrona M., Siwiec E., 2012. Application of the CIE Lab model in research of fly ash colour. *Problemy Eksploatacji*, 3, 177–188 (in Polish).

Plataniotis K., Venetsanopoulos A.N., 2014. *Color image processing and applications*. Springer, Berlin, Heidelberg. DOI: 10.1007/978-3-662-04186-4.

Reynolds O., 1883. An experimental investigation of the circumstances which determine whether the motion of water shall be direct or sinuous, and of the law of resistance in parallel channels. *Phil. Trans. R. Soc.*, 174, 935–982. DOI: 10.1098/rstl.1883.0029.

Schönfeld F., Hessel V., Hofmann C., 2004. An optimised split-and-recombine micro-mixer with uniform 'chaotic' mixing. *Lab Chip*, 4, 65–69. DOI: 10.1039/b310802c.

Vega-Alvarado L., Taboada B., Hidalgo-Millán A., Ascanio G., 2011. Image analysis method for the measurement of mixing times in stirred vessels. *Chem. Eng. Technol.*, 34, 859–866. DOI: 10.1002/ceat.201000060.

Woziwodzki S., 2014. Mixing of viscous Newtonian fluids in a vessel equipped with steady and unsteady rotating dual-turbine impellers. *Chem. Eng. Res. Des.*, 92, 435–446. DOI: 10.1016/j.cherd.2013.09.013.

Received 03 April 2021
Received in revised form 07 November 2021
Accepted 10 November 2021